



Optimization of the solar energy storage capacity for a monitoring UAV

Franklin Salazar^{a,d,*}, Maria Sofia Martinez-Garcia^b, Angel de Castro^b, Nube Logroño^c,
Maria F. Cazorla-Logroño^c, Jesús Guamán-Molina^d, Carlos Gómez^b

^a Departamento de Doctorado, Universidad Autónoma de Madrid, Madrid, 28027084 Spain

^b HCTLab Research Group, Universidad Autónoma de Madrid, Madrid, 28049, Spain

^c Escuela Politecnica de Chimborazo, Riobamba, Ecuador, 60155, United States

^d Faculty of Engineering in Electronic and Industrial Systems, Technical University of Ambato, Ambato, Ecuador, 180103 United States

ARTICLE INFO

Keywords:

Battery
Flight autonomy
PV System
Storage
UAV

ABSTRACT

Unmanned aerial vehicles integrate propulsion systems, communication modules, and sensors, allowing an operator to perform autonomous or remote-controlled flight actions. UAVs provide important advantages for exploring remote locations due to their cost-effectiveness and versatility compared to manned aircraft. However, addressing safety and flight autonomy challenges remains necessary. This paper analyzes and proposes the integration of a photovoltaic solar system to power UAV devices. Through a brief analysis of the aerodynamic model and the wing profile, a consolidation of the solar cells has been achieved without compromising efficiency in-flight maneuvers. Furthermore, an analysis is conducted on the potential of using photovoltaic solar resources in fixed-wing aircraft. The research aims to determine the optimal wing surface area required for video surveillance applications. The current model under discussion is a glider-type system that incorporates two distinct systems, one for video transmission and the other for telemetry data acquisition. An analysis of the battery charge and discharge pattern was carried out using computer simulation tools. This analysis aimed to optimize the battery charging process by integrating photovoltaic cells. The results and conclusions of the tests are described in the final section of the paper.

1. Introduction

Aircraft are playing an important role in different activities, where important algorithms are increasingly being developed that allow their remote operation in very diverse environments and specific areas such as precision agriculture, infrastructure, and environmental monitoring, video surveillance, topography [1,27]. The development of this technology makes it possible to currently have unmanned aerial vehicles (UAVs) for wide use. The effective operation of these systems demands a degree of flight autonomy, which highlights the scientific and technological interest in extending that time horizon [2]. It is also necessary to mention that some larger or longer-range unmanned aerial vehicles (UAVs) utilize internal combustion engines that are comparable to those found in fuels. Consequently, there is a substantial demand for an unlimited and renewable source of energy for aircraft propulsion [20]. Solar energy represents one of the available renewable sources that can be harnessed to increase the flight time of UAVs without significantly

increasing the weight by increasing the size of the fuel system [3]. The flight range of a UAV can vary significantly and depends on several factors, such as the design of the UAV, the type of motorization, the weight of the payload, the weather conditions and the type of mission. Some smaller and lighter UAVs can have only a few minutes of flight range, while other larger and more advanced UAVs can fly for hours or even days [2,4,25]. Smaller electric UAVs, such as consumer drones, generally have a flight range about 10 and 30 minutes. These UAVs are limited by the capacity of their batteries, and as it increase in size and payload, the flight range is reduced due to increased power consumption. On the other hand, larger UAVs for professional or military use, such as fixed-wing vehicles or long-range drones, can have a much wider range. Several researchers have ventured into creating robust systems by using batteries and energy charge and discharge controllers, but the weight of the aircraft inevitably increases. This is how several projects have recently been developed to integrate renewable energies into the surface of aircraft, with the aim of increasing flight autonomy [5–7,

* Corresponding author.

E-mail addresses: franklin.salazar@estudiante.uam.es (F. Salazar), sofia.martinez@uam.es (M.S. Martinez-Garcia), angel.decastro@uam.es (A. Castro), nubelogrono83@gmail.com (N. Logroño), maria.cazorla@epoch.edu.ec (M.F. Cazorla-Logroño), jguaman0585@uta.edu.ec (J. Guamán-Molina), carlosq.gomez@uam.es (C. Gómez).

<https://doi.org/10.1016/j.sfr.2023.100146>

Received 14 August 2023; Received in revised form 23 November 2023; Accepted 15 December 2023

Available online 21 December 2023

2666-1888/© 2023 Published by Elsevier Ltd. This is an open access article under the CC BY-NC-ND license (<http://creativecommons.org/licenses/by-nc-nd/4.0/>).

28–30]. To estimate the energy needs and environmental impacts associated with UAV flight time, we first modeled the energy demand and performance of the drones. Solar panels have been integrated into some UAVs to provide additional power or even be the main source of power to supply on-board systems. The advantage of using photovoltaic modules is that they can be attached to the UAV fuselage to obtain solar energy during aerial operation. This additional energy is used to charge the on-board batteries, extending the UAV's flight range. By capturing solar energy during the day, the UAV can harness it to power its systems and reduce reliance on internal batteries [6]. In some cases, solar panels can directly power the systems and equipment on board the UAV, without the installation of additional batteries. This can be useful on UAVs that require a continuous power source and do not have significant weight restrictions. Solar panels can provide the power needed to operate cameras, sensors, or other equipment. By using solar panels as a direct power source to generate power during the flight, the load on the UAV's batteries can be reduced. This can help extend battery life by reducing the number of charge and discharge cycles, which in turn reduces the cost and environmental impact associated with frequent battery replacement. When incorporating solar panels into UAVs, it is imperative to consider their design, which includes the size, weight and placement of the panels. It is critical to find a balance between the surface area of the solar panels needed to capture sufficient solar energy and the potential effects on the UAV's performance and aerodynamics. It is important to note that the amount of solar power available can vary based on weather conditions and geographic location. UAVs that rely solely on solar power can face challenges in areas with little sun exposure, in harsh weather conditions, and at night. Therefore, in many cases, solar panels are used in combination with batteries to ensure a constant power supply. The use of a storage system in low power photovoltaic systems is essential to provide a regulated energy delivery that allows the proper operation of each of the electronic components of the UAV. Based on the construction characteristics of the various types of aircraft, fixed-wing aircraft are one of the most used for the implementation of solar cells on their surface due to their aeronautical design [8]. This type of aircraft also has a low energy consumption compared to multirotor aircraft, so the various ways of extending the flight range for fixed-wing aircraft are analyzed, since their physical characteristics enable them to glide at different altitudes with a minimum of energy. For the implementation of solar cells on aircraft, highly variable natural factors such as solar radiation and temperature are analyzed; that model solar energy for aircraft propulsion. On the other hand, the main contribution achieved in this research is the application of an optimization algorithm to control the energy consumption of the aircraft based on the different flight profiles [9,10].

One of the main contributions of this article is the increase in the autonomy of the designed UAV, by incorporating a photovoltaic solar energy backup system. The optimization of the storage system is carried out based on an objective function, in which the battery capacity is minimized to increase flight autonomy, since it has a direct relationship with the weight of the aircraft. On the other hand, the appropriate design of the aircraft allows the different components to be integrated to monitor large areas. The analysis of the different types of wings, tails and fuselage has allowed us to determine the one that best adapts to the flight conditions of recognition and monitoring of the UAV. The simulations of different flight routes based on the determined models have made it possible to reduce the costs associated with the flight tests carried out since the designs are validated in simulation form to move on to construction. This article consists of three sections. The first section presents the introduction in which the importance of the research is addressed as well as a brief review of the most relevant studies on the subject. The second section presents the materials and methods used for the development of the article. In this section the variables prior to the design and sizing of the UAV are analyzed, as well as the optimization of the system to improve the flight performance of the UAV. This validation is performed by simulating different flight trajectories. In the results

section, the evaluation of the battery charging and discharging behavior is presented using flight profiles of real conditions, allowing to analyze the increase of the UAV's flight capacity by incorporating the photovoltaic system as the main component of the UAV's flight performance.

2. Materials and methods

2.1. Development of the UAV prototype

This paper describes the use of a fixed-wing aircraft associated with video surveillance actions. Video surveillance systems are made up of a group of optical sensors that perform vision of defined areas. In this sense, agricultural fields stand out in whose application the variables to be monitored are defined, which through different sensors acquire information from these environments. Another example is topographic planimetric surveys, where aircraft are required to have a high flight autonomy and obtain great results. These images can be processed to generate alarms, interpret scenes and make decisions automatically [11]. For the conceptualization and sizing of the UAV, a detailed study of the meteorological conditions of the area in which the prototype flight tests were carried out was carried out [23]. The sector has an average temperature of 18 degrees with a probability distribution centered between 18 and 22 degrees Celsius. Fig. 1 shows the average temperature data for the last three months obtained from the control tower of the Chachuan airport. Fig. 1.b also shows the probabilistic distribution of the last years of record. In the Fig. 1.c shows the whisker diagram of the temperature in which it can be observed that the lower end is approximately at a temperature of 9°C.

The wind rose of the flight site is presented in Fig. 2 based on the measurements obtained from the Chachuan Airport. As can be seen in Fig. 2, it can be noted that the wind in the area is predominantly in a north-westerly direction, with winds of up to 2.5 m/s at a height of 20 m, which indicates that speeds of up to 3.8 m/s at 300 m will be available by interpolation of Hellmann's exponential law [22].

The wind rose, also called a nautical rose or air rose, is a circular representation of the direction and frequency of the wind in a specific geographic region. In this way, we proceed to graph the data extracted from the Chachuan Airport as base parameters for navigation and performance of the UAVs. It is recommended to make the graph of the wind rose before the flight of UAVs, allowing a better performance of the aircraft before planned routes. As can be seen in the figure, the concentration of the wind flow is located in the Northwest of the Chachuan Airport. This information allows the pilot to estimate the stability of the UAV against gusts of wind coming from that direction. In autonomous flight missions, wind gusts from that direction must be considered to avoid aircraft stability problems.

To obtain a clear view of the wind speed distribution in the sector, the adjustment to a Weibull distribution was performed, which is a fundamental part for the parameterization of the wind model for the study of the aerodynamic profile behavior. Fig. 3 shows the adjustment of the distribution with which it can be observed that in the sector there is a great variability of the speed, however the highest concentration of wind speeds is centered between 1.5 and 2.5 m/s, allowed to have a better view of the wind model for the aerodynamic analysis. There is a wide variety of UAVs configurations, and their profiles vary individually or totally according to their application characteristics [12].

In the first instance, the application of the UAV must be analyzed, for this investigation a glider at low speeds is treated. Thus, the process for the design of the wing profile is described in order to achieve an efficient geometry for the specific case of Ambato.

This implies that the airfoil model must have a low Reynolds number. Normally, the Reynolds number determines the flow of a fluid. In this sense, for glider-type UAVs, there is a range of 250,000 to 700,000, which implies reaching speeds of 14 m/s to 40 m/s. As it is a fixed-wing UAV for mutinous applications, low-altitude flight tests that do not exceed 300 m high are considered.

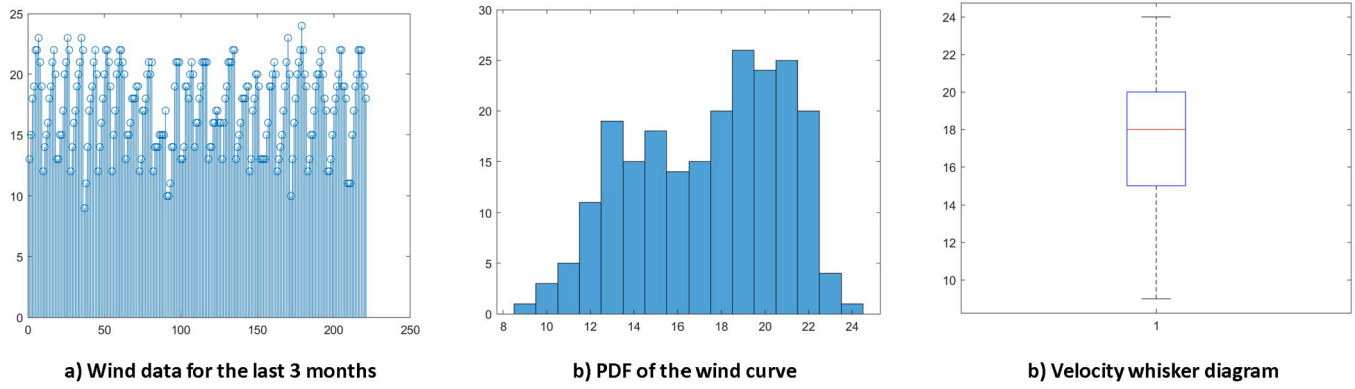


Fig. 1. Flight environment temperature.

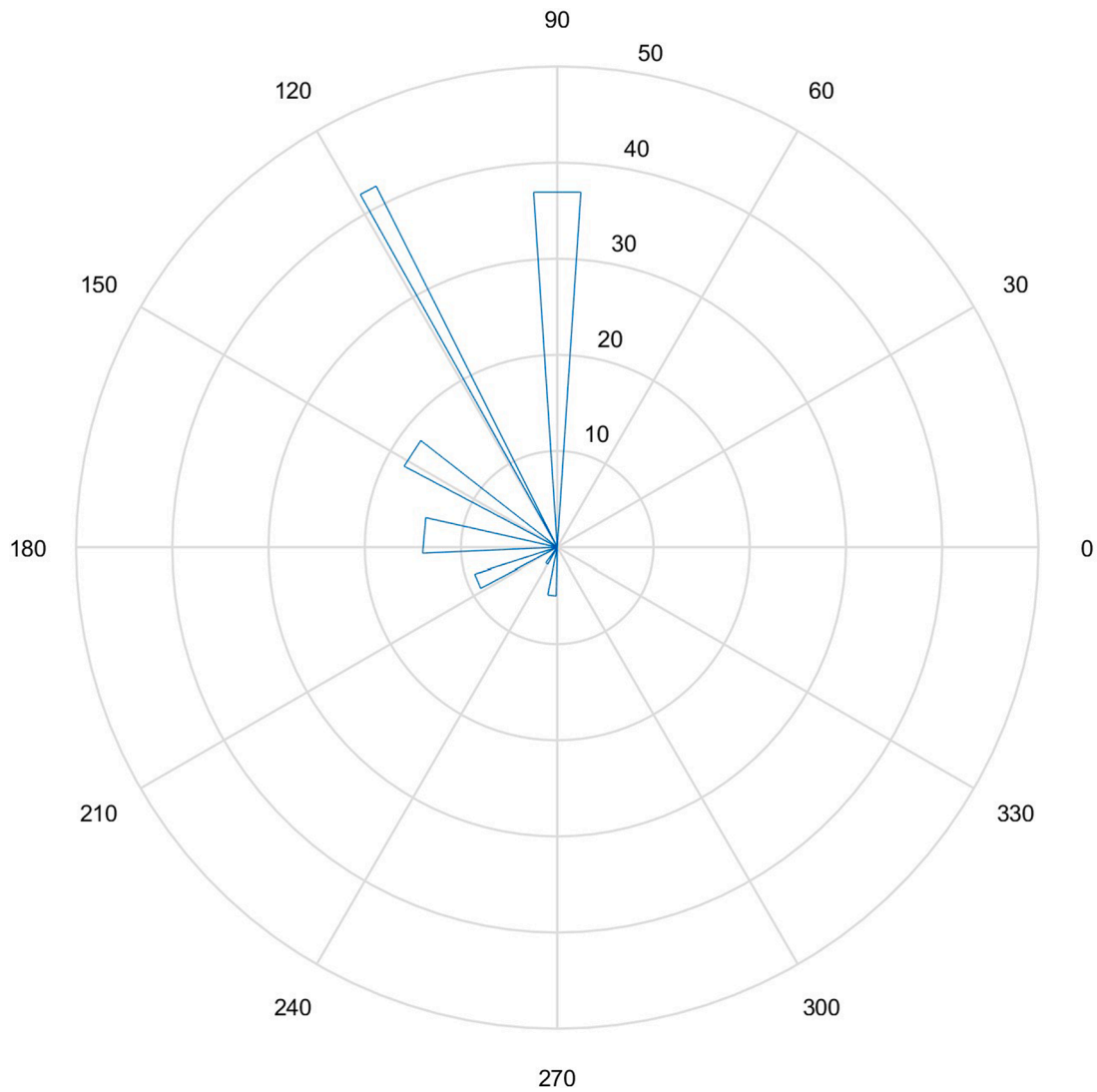


Fig. 2. Wind rose.

For this, the FoilSim III tool, developed by NASA's Glenn Research Center, has been used. This tool It allows computes the theoretical lift and drag of a variety of airfoil shapes. The program includes a stall model for the airfoil, a model of the Martian atmosphere, and the ability to specify a variety of fluids for lift comparisons. The main parameters used for the simulation are presented in [Table 1](#).

Based on the weight of the camera, the average speed that the UAV can achieve on estimated missions of 14 km/h, a Reynolds number based on the average wing aerodynamic chord of approximately 250,000 was chosen. The airfoil is characterized by a high pitch and a high pressure gradient along its chord, making its low Reynold number suitable for tracking and video surveillance missions. The most suitable aspect ratio

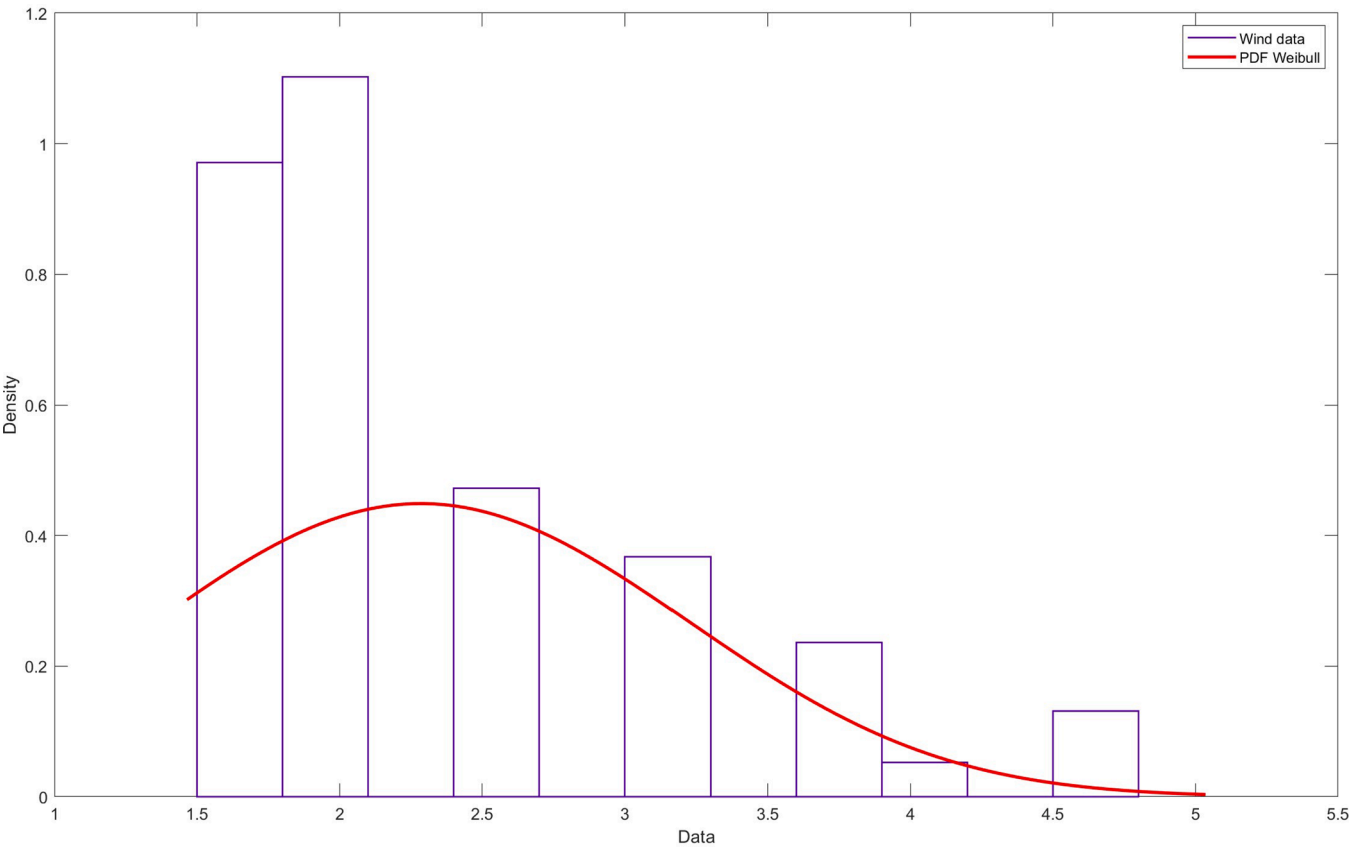


Fig. 3. Wind speed probability curve fitting.

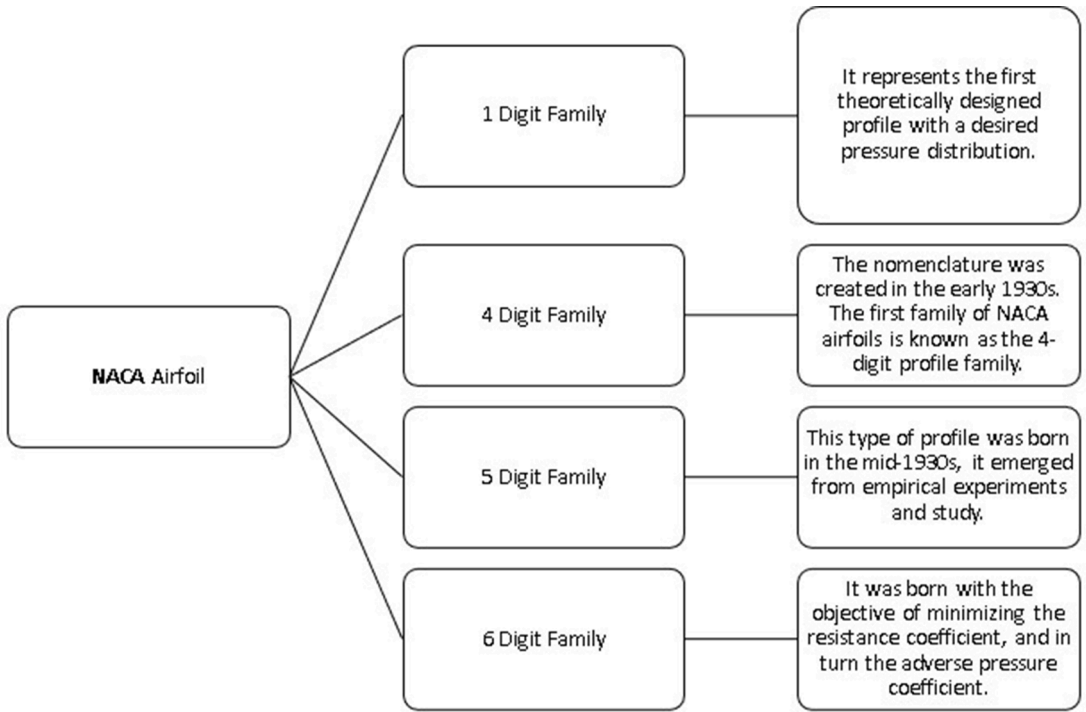


Fig. 4. CFD simulation of the airfoil.

(AR) for the UAV wing is of utmost importance. Finding a high AR value for the UAV allows for better performance, keeping resistance and power losses to a minimum, in addition to obtaining a suitable surface

for installing the photovoltaic generation source. Taking into account, there is a great variety of UAV configurations and their profiles vary according to their application.. The aircraft profile calculations are

Table 1
Environmental Considerations for Flight Tests.

Study Variables	Values
Wind Speed	3.8 m/s
Altitude	300 m
Wind Density	1.191 kg/m ³
Drag Coefficient	0.025
Flight Temperature	139°C
Pressure	97.71 kPa

carried out in stable flight conditions, thus seeking stability between the design conditions carried out [36]. Table 1, presents the different wing aerodynamic profiles that have been discussed in recent years. Each of the profiles studied present certain characteristics that make them ideal for the design of different UAVs [37].

Table 2 presents the classification of UAVs, according to their type of wing, which presents the physical and operating characteristics of the UAVs [32].

2.2. Aerodynamic study

The fundamental characteristic for the aerodynamic performance of a UAV is its wing profile because it has a great influence on its behavior [35,38]. The main performance characteristic of a wing is to generate lift within an incident current to maintain control of the aircraft and its operation in an agronomically efficient manner [35]. The wing profile and its nomenclature NACA (National Advisory Committee For Aeronautics), which defines the geometric concept of a wing profile based on tests carried out in wind tunnels that have allowed them to be defined [39,40]. Fig. 3 shows a classification of the NACA wing profile families.

The Reynolds number allows the design of the aerodynamic surface of the UAV, and is defined in the wing chord R as Eq. 1.

$$R = \frac{Vc}{\nu} \quad (1)$$

Where: V is the flight speed (TAS or true speed), c is the length of the wing chord and ν is the kinematic viscosity of the fluid in which the airfoil operates, which in our case is 1.460×10^{-5} m²/s for the atmosphere at sea level.

The span and mean chord values are essential data for the calculation of the wing area [32]. The wing area (S) can be calculated from Eq. 1, which represents the wing loading (CA) [32].





$$CA = \frac{WT}{S} \quad (2)$$

Where: WT is the weight of the total UAV S is the wing surface. Solving the surface, Eq. 3 is obtained.

$$S = \frac{WT}{CA} \quad (3)$$

Taken into account that the wing loading can be obtained from the

Table 2
Types of wing profile.

Profile Type	Characteristic	Graphic
Planoconvex Profile	Straight bottom surface and curved top surface	
Concave-Connected Profile	Inward curved soffit	
Symmetrical Biconvex Profile	Equal intrados and extrados curves	
Supercritical Profile	Narrower inwardly curved soffit	

Eq. 4.

$$CA = C \cdot \sqrt{S} \quad (4)$$

Substituting the wing loading into Eq. 3 of the surface is obtained:

$$S = \frac{WT}{C \cdot \sqrt{S}}$$

Solving the wing surface, Eq. 4 is obtained.

$$S = \sqrt[3]{\left(\frac{WT}{C}\right)^2} \quad (5)$$

The wing loading coefficient depends on the type of aircraft that is designed for construction; the loading coefficients are presented in Table 3 [32].

The designed UAV presents a trainer-type application being the basis for future research. The weight of the unmanned aerial vehicle will depend on all the components on which the UAV will be built. For this, all the components that will be used in its manufacture are described in order to have an approximate payload [33]. The total weight of the aircraft is calculated using Eq. 5.

$$WT = W_{cabin} + W_{wall} + W_{tail} + W_{motor} + W_{battery} + W_{utilload} \quad (6)$$

Replacing each of the values we obtain

$$WT = 262g + 1972g + 316g + 240g + 602g + 1184g \quad WT = 4576g$$

Applying the wing loading coefficient (C) of 6, which corresponds to a training aircraft, in Eq. 4 we obtain S .

$$S = \sqrt[3]{\left(\frac{4576}{6}\right)^2}$$

$$S = 83.47502 \text{ dm}^2$$

$$S = 8347.502 \text{ cm}^2$$

The wingspan of the airplane (b) which is given by the maximum distance of the wing, measured from wingtip to wingtip, regardless of shape, based on aspect ratio (AR), Eq. 7.

$$AR = \frac{b^2}{S} \quad (7)$$

Solving for the wingspan of the UAV (b) we obtain Eq. 8.

$$b = \sqrt{S \cdot AR} \quad (8)$$

To obtain an elongated appearance of the UAV, an aspect ratio (AR) of 14 has been chosen, taking into account initial data referring to the antecedents of aircraft developed. With what you get:

$$b = \sqrt{8347.50 \cdot 14}$$

To calculate the value of the middle chord (c), Eq. 9 is used:

$$C = \frac{S}{b} \quad (9)$$

Replacing the values in Eq. 8, we obtain:

$$C = \frac{8347.50}{342}$$

$$C = 24.41 \text{ cm}$$

$$C = 244$$

Taper ratio (λ) is defined as the ratio between the tip chord (C_t) to the root chord (C_r). To have a stable lifting surface, the taper ratio (λ) was taken, which is 0.7, because this value allowed having a stable lifting surface, for the calculation of the tip chord, the same one that is calcu-

Table 3
Classification of UAVs.

Classification	Physical Characteristics	Operation Features
Fixed wing	They require a runway to land.	Long resistance.
Rotary wing	Helicopter Type Possibility of vertical takeoff and landing.	High maneuverability.
Hot air balloons	High maneuverability.	Lighter than air, and usually large in size.
Flapping wings	Small and flexible morphological wings. They can have hybrid configurations.	Long endurance.

lated by the Eq. 9:

$$\lambda = \frac{C_t}{C_r} \quad (10)$$

With which you get:

$$C_t = \lambda \cdot$$

$$C_t = 0.7 \cdot 244 \text{ mm}$$

$$C_t = 170.8 \text{ mm}$$

For this project, a 2-degree dihedral was implemented, considered on a high wing, with the purpose of having a greater surface area for the incorporation of solar cells that allow energy to be delivered to the power system [34],[35].

The wing design concluded with the estimation of the optimal taper ratio that would result in an elliptical approximation of the wing. It was found to be 0.7 for the chosen $AR = 14$, combined with S4083 wing profile, shown in Fig. 5. The semi-conical plant offers the possibility of easy and practical transport of video surveillance elements and equipment. The most relevant characteristics of the aerodynamic design are presented in Table 5 [24].

2.3. Wind flow simulation

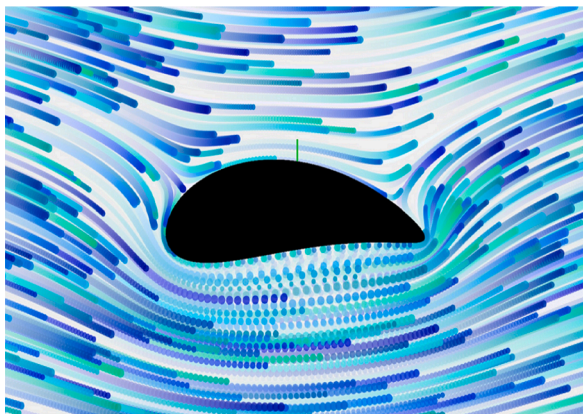
In addition, through a complex analysis, the wind flow can be appreciated with different simulations, which allows the wing model to be adequate for the weather conditions of Ambato. At this point it is important to note that the geography allows you to experience very varied wind levels due to the presence of the Andes mountain range, you can see wind flows in different directions. In Fig. 5, it is visualized how the wind flow surrounds the wing profile and an idealized aerodynamic model for an airplane is obtained.

Once the wing profile has been defined and its behavior analyzed in different wind flows, it is important to check its behavior based on the following factors:

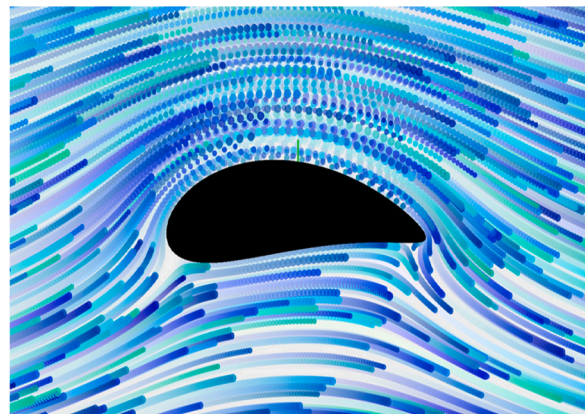
- Polar Drag C_d vs C_l .
- Aerodynamic performance C_l/C_d vs angle of attack.
- Lift coefficient C_l vs angle of attack.

In the first place, the polar drag is analyzed, which is a factor that relates the coefficients of drag and lift. In Fig. 6, the polar drag is presented, the same one that is graphed symmetrically since in the model an angle of attack of 0 degrees has been considered.

Subsequently, progress is made with the study of the aerodynamic characteristics. It can be seen that the initial angle of incidence is zero degrees, however, it can fluctuate in a range of -10 to 10 degrees, as illustrated in the corresponding Fig. 7.



Takeoff wind flow



Landing wind flow

Fig. 5. CFD simulation of the airfoil.

Table 4

Main characteristics of the wings.

C	Airplane Model
2-3	Airplane Model
4-5	Motogliders
6-8	Coach
9-12	Acrobatic
13-15	Races

Table 5

Main characteristics of the wings.

Angle of sweep	09°C
Wing planform area S_W (m ²)	0.834
Root chord length c_r (m)	0.224
Tip chord length c_t (m) 0.15	0.170
Taper ratio λ_w	0.7

Simulations and aerodynamic analyses provide a number of assumptions that are not all given in actual testing, but it is important to do so prior to aircraft design. First, it is important to know the application and the power consumption that the aircraft will require. In this way, the optimal design of the UAV will be analyzed to integrate a solar photovoltaic system to supply energy to its integrated systems [13]. Table 6 presents a summary of the systems mounted on the proposed UAV, where its elements are described with their main characteristics.

It is important to mention that together the telemetry and video system represent a current consumption of 1117 mA.

In addition to the video and telemetry systems, the aircraft will integrate a propulsion system made up of a QA2825 engine, while the direction will be controlled with DS-843MG servomotors. The consumption of these elements is covered by a battery arrangement that, through a balance module, performs the actions of charging and discharging energy. In this sense, it is capable of detecting overloads and taking advantage of the energy supply captured by the solar cells, through a voltage regulator. In Fig. 8, the different elements of the UAV can be seen, as well as their communication interfaces and the operating voltage levels for each one.

A fixed-wing UAV model has been chosen in which the aforementioned elements can be integrated, likewise, the aerodynamic model has been made and its flight behavior validated [14]. Aircraft profile calculations are performed under controlled flight conditions, thus seeking stability between the design conditions performed. The fundamental characteristic for the aerodynamic performance of a UAV is its wing profile, because it has a great influence on its behavior [14]. To determine the appropriate profile, the main coefficients were evaluated for an

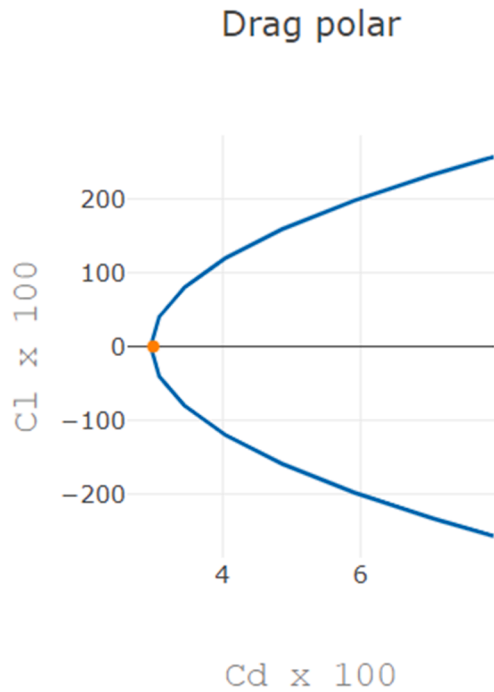


Fig. 6. Polar Drag.

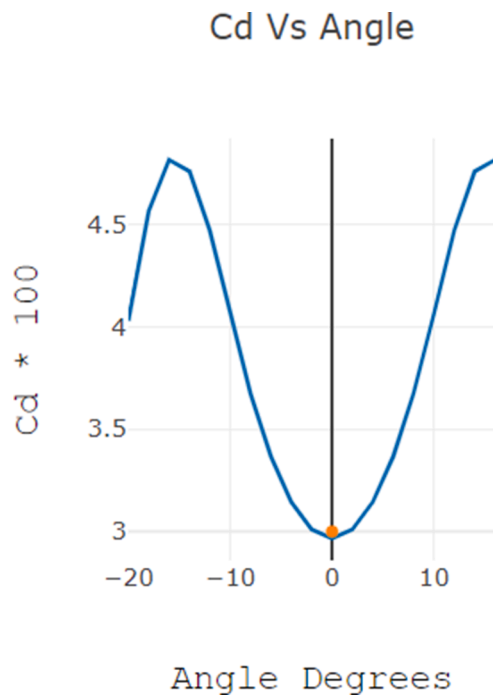


Fig. 7. Aerodynamic performance.

angle of attack of zero degrees [15]. In the present work, the optimization of the flight autonomy of a fixed-wing UAV is addressed. For the specific case of Ambato - Ecuador, different wing profiles were analyzed, where the S4083 model stands out, which presents a glider-type configuration. Also, an extensive wing surface will be available for the integration of solar cells as a generation system for the aerial platform. Sustainability by moving through the air in one direction for long periods of time is ideal for use in monitoring and video surveillance

Table 6

Main characteristics of the systems that make up the proposed UAV.

UAV Systems	Elements	Characteristics
Telemetry System	Auto Pilot - Pixhawk 2.1	Processor: STM 32F427 32bits. Voltage: 4.1 to 6 V. Weight: 75 gr.Interface: I2C, UART, CAN.
	Radio 3 DR	Frequency: 915 Mhz.Interface: TTL UART. Protocol: Mavlink. Sensibility: -167dBm.
	GPS-Radiolink M8N GPS SE100	Voltage: 1.65 to 5 V. Power: 50mA. Channels: 72.
Video System	Wind Speed Sensor - Holybro	Voltage: 3.3 to 5 V. Power: 150 mW. Resolution: 0.84 Pa. Interfaces: I2C, SPI.
	Camera GoPro Hero 6 Black	Firing Angle: 150° Battery: 1220 mAh. Interfaces: USB 2.0, HDMI. Weight: 118 gr.
	Video Transmitter - Herelink	Voltage: 7 to 12 V. 2 MMCX antenna connectors Signal transmission and communication

applications. This profile allows for a large wing area and has a low Reynolds number with a maximum thickness of 8% at 22.5% chord and a maximum camber of 3.4% at 35.5% chord. The evaluation of the coefficients of lift (CL), coefficient of drag (CD) and coefficient of moment (CM) of the Seling S4083 airfoil, present adequate performance for use in different scenarios. The rear stabilization of the aircraft is one of the main features to provide the UAV with mobility. Proper selection of the tail type is a crucial detail for UAV control and flight. The stabilizer known as inverted T type, allows to have a lower weight and lower drag force, so this stabilizer is the most suitable for the research design. The weight of the unmanned aerial vehicle will depend on all the components that will integrate the UAV, the same ones that are detailed in Table 7.

In Table 8, the measurements of the UAV proposed in the present investigation are presented.

2.4. Construction and testing of the prototype

It is important to take into account the optimal length between the fuselage and the tail of the airplane, which is 1.55 m, for which a volume coefficient of 0.6 was considered, with a UAV correction factor of 1 based on a typical geometry, Tadpole Shape. There is a maximum coupling between tail and fuselage of 3.5 cm. Thus, the 3D design of the UAV is carried out, using the AutoCAD software, in Fig. 9, the final model of the UAV can be seen based on the aforementioned wing profile.

The 3D design is exported in STL format for rendering in the Blender software, which allows its import to the MatLab software. The robustness of the aerodynamic design of the UAV is evaluated through the MATLAB software in which different flight paths are programmed. Proceeds to carry out the functions for the rotation and translation movement of the aircraft in three dimensions according to the MATLAB environment. The objective of the control is to obtain the positions that are applied to the UAV, positioning the UAV in x,y,z coordinates and a desired orientation, where the UAV has characteristics of an omnidirectional robot, that is, it can move in any direction, in addition, it has the three angles of inclination that are the roll, pitch, and yaw. In addition, it is used a Jacobian matrix that allows representing the relationships between two sets, one corresponding to input variables and the other to output variables [16]. Where each element of the matrix represents the value of the partial derivative of an output variable with respect to a specific input variable. The Jacobian matrix for the proposed model is presented in the equation (10). The control process described uses the Jacobian matrix, made up of the position and orientation errors, in addition to a control matrix to calculate the position and orientation reference. Based on this reference, the control actions to be applied to the UAV are assigned. Through the updates of the orientation angle and the linear speeds, the following of the desired trajectory and the evolution of the positions of the UAV in time are achieved.

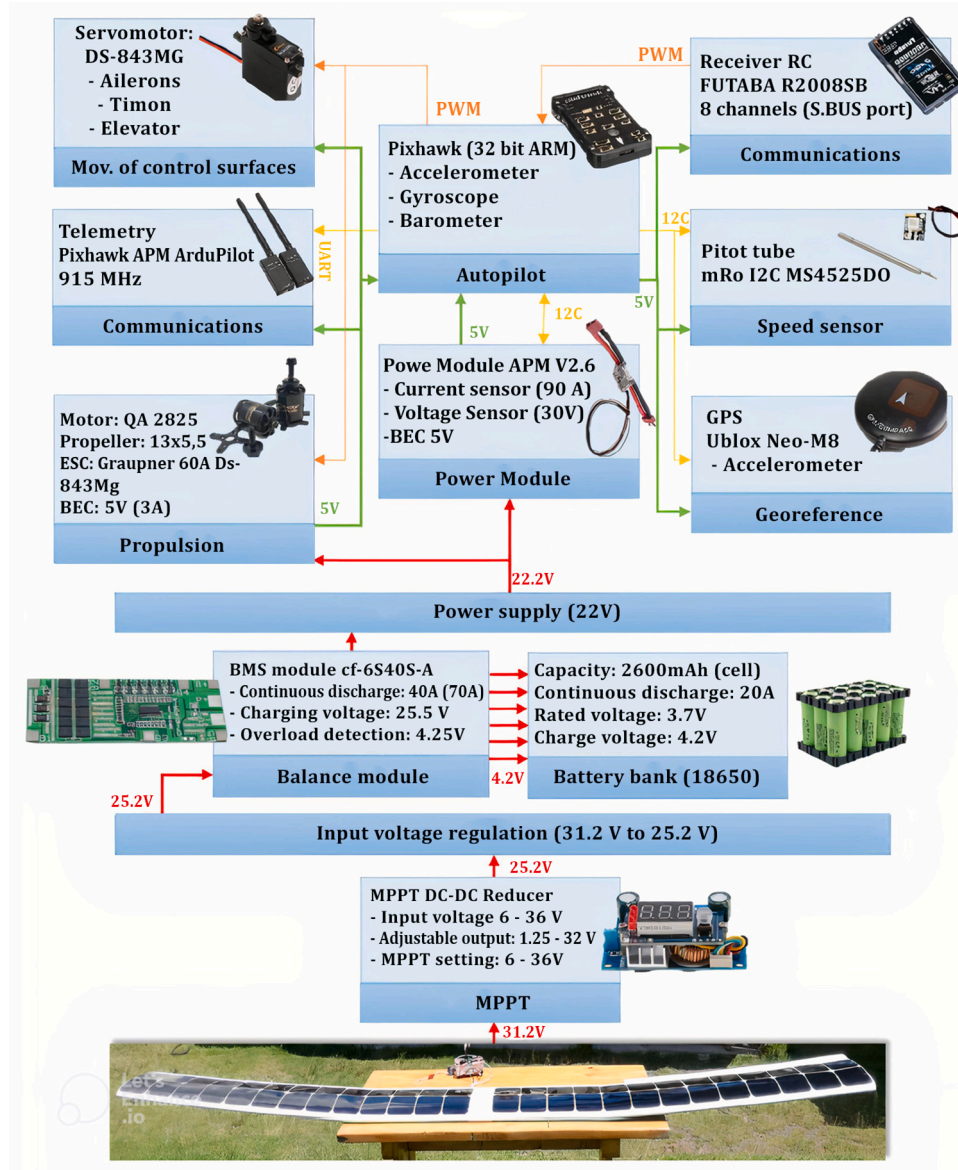


Fig. 8. Elements and Interfaces of the proposed UAV.

Table 7

Weight of UAV components.

UAV Components	Weight (g)
Cabin	262
Wing	1972
Tail	316
Battery	602
Motor	240
Camera	118

Table 8

Summary of the dimensions of the proposed UAV.

UAV Components	Dimensions
Wing Surface	8347.50 cm ²
Wingspan	342 cm
Middle rope	24.41 cm
Tip rope	17.08 cm
Dihedral	2 degrees (for high brim)
Fuselage Length	97.6 cm
Fuselage height	8 cm
Fuselage width	7cm

$$\dot{\mathbf{X}} = \begin{bmatrix} \dot{X}_a \\ \dot{Y}_a \\ \dot{Z}_a \\ \dot{\varphi}_a \end{bmatrix} = \begin{bmatrix} \cos(\varphi_a) & -\sin(\varphi_a) & 0 & 0 \\ \sin(\varphi_a) & \cos(\varphi_a) & 0 & 0 \\ 0 & 0 & 1 & 0 \\ 0 & 0 & 0 & 1 \end{bmatrix} \begin{bmatrix} V_{ax} \\ V_{ay} \\ V_{az} \\ W_{az} \end{bmatrix} = \mathbf{J} \quad (11)$$

The simulation of various trajectories based on the kinematic model is depicted in Fig. 10. The figure illustrates a straightforward representation of the tracking error using Matlab examples. Four trajectories are shown where programmed UAVS routes in the Matlab environment. The red line represents a percentage error in the flight stability of the

UAV, while the blue line represents the determined trajectory. Testing route is demanding to UAV tracking stability in curves zones. And circular route show the minimum percent of error in programming routes. It is critical to note that UAV route tracking involves many considerations, such as navigation system accuracy, obstacle avoidance, UAV performance, and overall safety of operations. It is recommended to follow good engineering practices and extensive testing before implementing route tracking in a real operating environment.

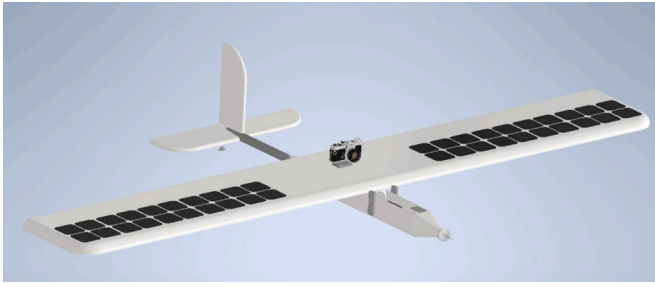


Fig. 9. Prototype model in AutoCAD.

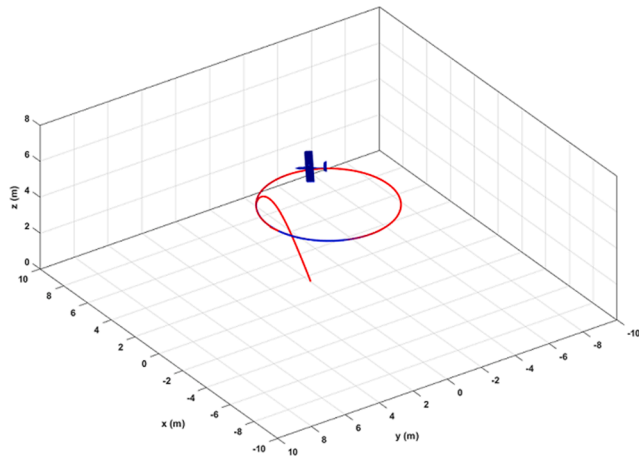
Unmanned aerial vehicles make it possible to monitor areas that are difficult for humans to access, their mobility is highspeed and they collect information that allows processes to be optimized. The following paragraphs describe the energy consumption of the proposed aircraft that integrates a photovoltaic power system together with an energy optimization algorithm based on different flight profiles is analyzed.

2.5. Energy consumption of the aircraft

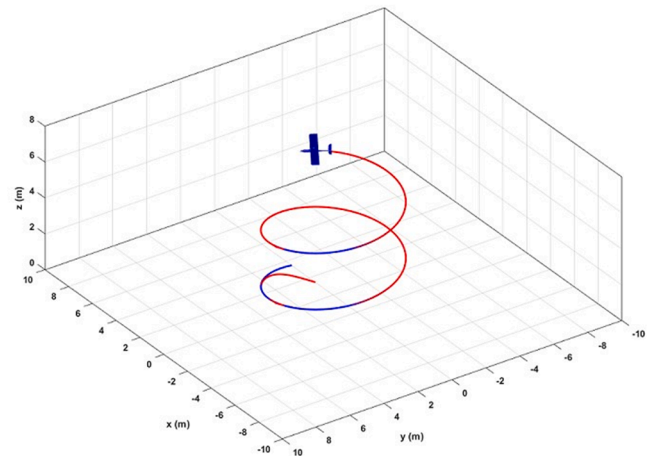
In an electric UAV, the propulsion system is made up of a number of

components. These include the electronic speed controller, motor, and propeller. Each of the components contributes to a loss of efficiency, ultimately converting electrochemical energy into mechanical work that propels the aircraft [2]. That is the reason why the main concerns in the deployment based on UAVs are the limitations and restrictions of their batteries. The same ones that must be charged at charging points connected to the electrical network, which in turn generates an extra cost. There are some cases which there is no availability to connect to an electrical network, especially in rural areas. To address these challenges, renewable energy sources (RES), such as solar photovoltaic (PV) systems, can be deployed to supply UAV charging sites in rural areas [17]. For the correct operation of the aircraft, it is important to establish a balance between energy consumption and its generation [18]. Additionally, to guarantee optimal operation of the aircraft propulsion system and maintain a rectilinear and level flight pattern, the implementation of an autonomous generation system is essential[5].

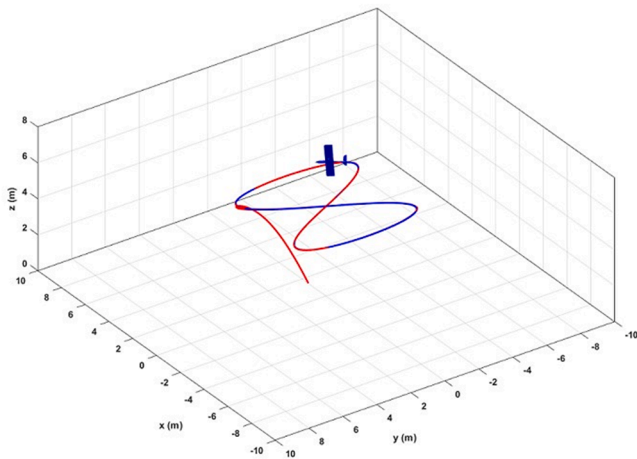
The UAV has integrated a photovoltaic generation system that supplies more energy when solar radiation falls on its surface. Peak sun hours are essential for the efficiency of systems that take advantage of solar energy, in this case for the UAV that directs that energy into its electronic systems. The term (HSP) "peak sun hours" refers to the period of the day in which solar radiation reaches its highest level, that is, the maximum intensity of sunlight. The specific schedule of the peak sun



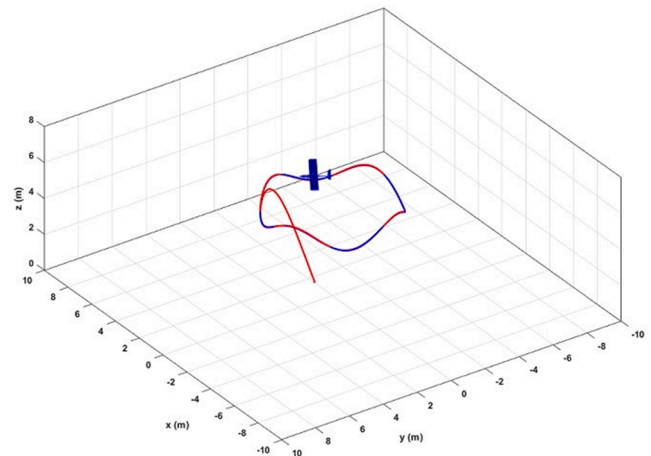
Circular



Helical



Eight



Testing

Fig. 10. Trajectory simulation in MATLAB of the proposed UAV.

hours may vary according to the geographical location, the season of the year and the climatic conditions. However, they usually occur around solar noon, which is when the sun reaches its highest position in the sky. This allows us to estimate around 4 HSP for the Chachuan airport. The number of solar cells is calculated using the Eq. 11 [21]:

$$N_T = \frac{E}{HSP * P_{mpp} * n_m} \quad (12)$$

Where:

E corresponds to the total daily consumption of the System,

P_{mpp} is the peak power of the solar panel and

n_m is the performance of the photovoltaic module considering the existing losses due to dirt, reflection, etc.

The photovoltaic solar generation system is made up of C60 photovoltaic cells, supplying the necessary energy to satisfy the energy consumption of the electronic systems used in aircraft. Therefore, this generation system can be used to connect auxiliary systems in the aircraft and minimize battery discharge. From another perspective, it is crucial to highlight that renewable energy generation systems for aircraft are still in the development phase. Consequently, the integration of these systems in UAVs presents challenges in the design, where a balance is sought between the weight and energy efficiency of the aircraft. The integration of solar cells in UAVs presents numerous advantages and disadvantages; a summary of the main advantages and disadvantages is presented in Table 9 [2].

Solar cells can be installed in unmanned aerial vehicles and thus take advantage of solar energy and thus provide an additional or in some cases main electrical generation system. In this sense, C60 solar cells with a yield of 0.9% were chosen for conditions in Ecuador, specifically Ambato. The monocrystalline cells have dimensions of 125x125 mm and are equipped with an aluminum bus bar. These cells reach a peak power output of 3.63 W and have an approximate weight of 6 g. An essential consideration in the research was the overall mass of the photovoltaic panels. Considering the structural characteristics of the panel, a plastic layer was incorporated to enhance the mechanical integrity of the individual cells. After the inclusion of this layer, the mass of each cell increased to 14 g. This weight includes the extra mass introduced by the welding connections between adjacent cells, a requirement for the assembly of the two photovoltaic modules situated on each wing. The total mass of these modules, inclusive of all associated components, amounted to 690 g.

Among the main characteristics of the C60 solar cells are:

- High efficiency in the conversion of sunlight into electricity, maximizing energy production in limited areas.
- Light weight due to the thin film design ideal for UAVs that need to maintain their payload capacity and flight capability.
- Flexible design ideal for integration into various parts of a UAV, such as the wings and the fuselage mainly.
- Continuous power generation for UAVs during their flight, extending their autonomy and minimizing dependency on batteries.

With this perspective, a renewable system consisting of 48 photovoltaic cells that will be located along the fixed wing of the UAV is consolidated [19]. In addition, due to the geometry of the aircraft, the

cells must be connected in series, thus reaching a power of 178.56 W. Fig. 11 shows the aircraft implemented with the photovoltaic solar generation system.

In the case of UAVs, batteries are the elements that must be taken care of the most since flight autonomy depends largely on them. In this sense, the renewable system is capable of supplying a peak current of 6 A under optimal atmospheric conditions. However, when conditions vary, a current of 1 A is reached on average. Furthermore, considering the weight of the aircraft, an average consumption of 20.01 Amperes has been calculated during flight operation. I hope this is what you are looking for.

3. Results

To evaluate the solar resource, it begins with the analysis of direct irradiation, which is obtainable through the PVGIS tool. This tool has an extensive database with meteorological information that facilitates the determination of an approximate total of 4.5 peak hours of sunshine in the province of Tungurahua, as illustrated in the corresponding Figure 12.

To calculate the power supply as well as the storage system, a Python programming was carried out and the flowchart is shown in Fig. 13. From the energy analysis, the average radiation and temperature data corresponding to the most critical month were acquired. These data are essential for calculating the battery capacity, as illustrated in the Fig. 14. However, in order to obtain the optimum capacity of the battery, the energy resource in the region was analyzed for one of the most critical days of the study month, which allows for obtaining the energy surplus that can be stored in the batteries [26].

The surplus generated by the photovoltaic system based on the system consumption allows the storage capacity to be determined. For this purpose, an objective function is proposed in order to optimize the battery capacity. The objective function is presented as a minimization of 1 of the power balance between the photovoltaic generation systems, PV_{power} and the load power, P_{load} and the battery, $P_{battery}$. On the basis of the objective function, as presented in the Eq. 12:

$$OF = \min \left\{ \text{abs} \left[\sum \left(\{ PV_{power}(T_{cell}, G) + P_{battery} - P_{load} \} \right) \right] \right\} \quad (13)$$

Taking into account the initial power of the installation, the optimization of storage capacity can be obtained as a result, Eq. 13 :

$$0.75 * iniPV_{energy} \leq PV_{power}(T_{cell}, G) \leq 1.25 * iniPV_{energy} \quad (14)$$

Where:

$iniPV_{energy}$ the initial energy obtained from deterministic calculation, generated by estimating the energy consumption using the PVsyst tool, based on panel temperature (T_{cell}) and direct radiation global (G). For this purpose, the following restrictions for the battery charging and discharging are considered $P_{UAV} \geq 0; \forall t$

Fig. 15 shows the block diagram of the proposed optimization.

The decision variables are subject to several non-negativity constraints expressed with the following equations (14), (15), (16) and (17).

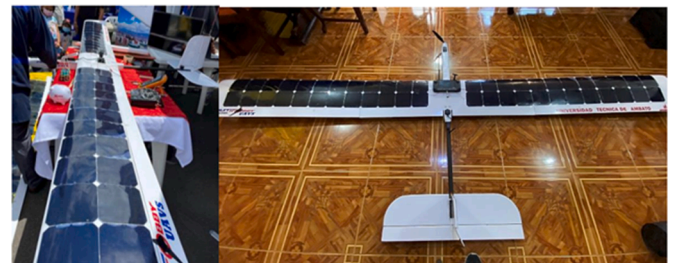


Fig. 11. UAV integrated with the Photovoltaic generation system.

Table 9

Advantages and disadvantages of the integration of solar cells in UAVs.

Advantages	Disadvantages
Clean and renewable energy source.	Limited energy storage.
Better autonomy of operation since the batteries can be charged during the flight.	Dependence on solar irradiation.
Minimization of weight by not using a deposit or tank for fuel.	High investment.
Lower noise ideal for video surveillance tasks where stealth is required.	

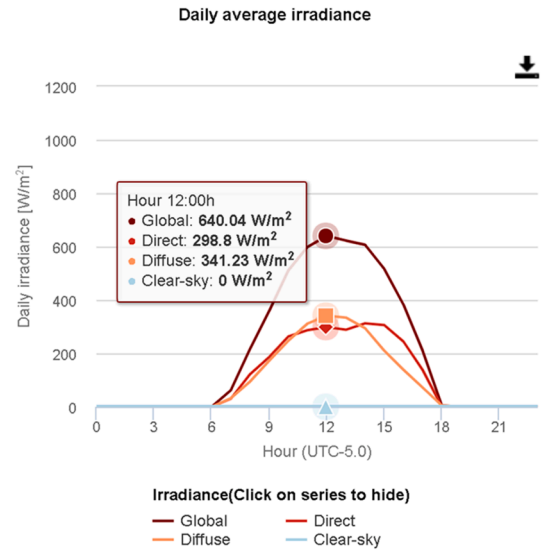
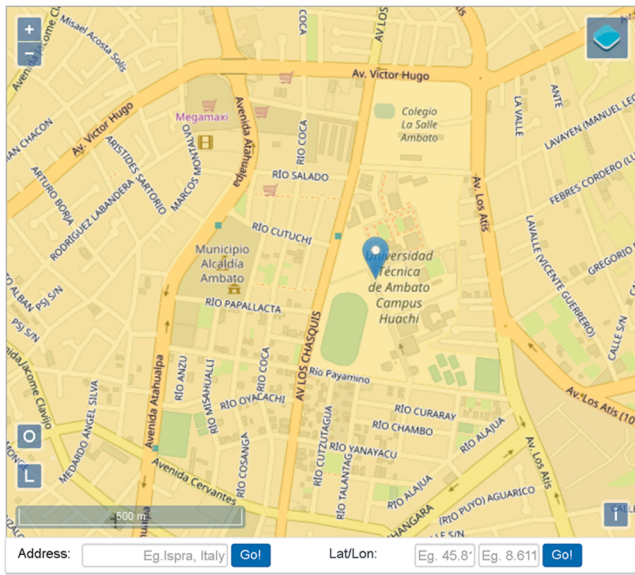


Fig. 12. Global irradiance of the study location.

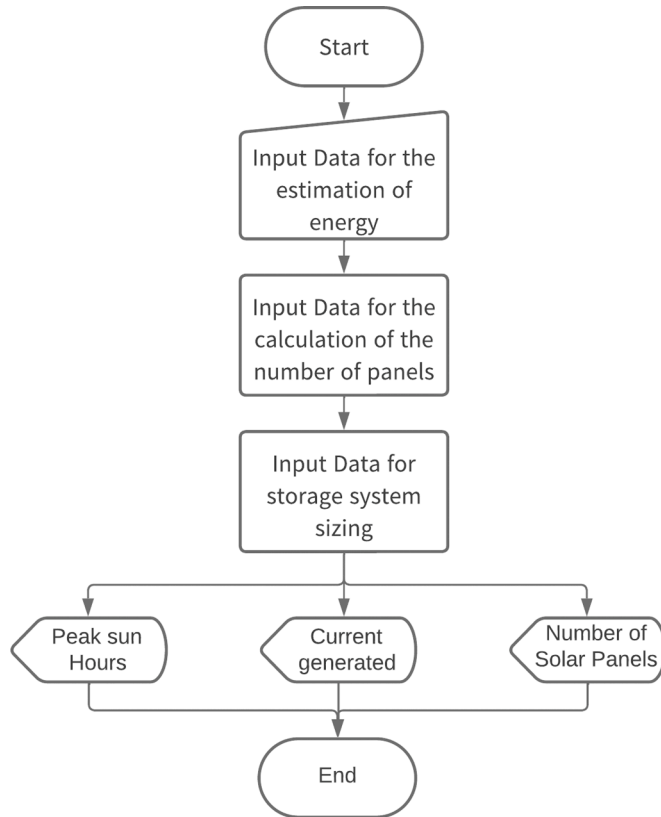


Fig. 13. Flowchart of PV and storage system design and sizing.

$$P_{pv-b}(t) \geq 0, \forall t \quad (15)$$

$$P_{pv-l}(t) \geq 0, \forall t \quad (16)$$

$$P_{b-l}(t) \geq 0, \forall t \quad (17)$$

$$SOC(t) \geq 0, \forall t \quad (18)$$

To ensure battery life, there are limits on the battery state of charge (SOC) and they are given by Eq. 18.

$$SOC_{min} \leq SOC(t) \leq SOC_{max}; \forall t \quad (19)$$

To optimize the system we worked with the pymo library of python, with which we determined an optimal capacity of 15 mAh. Once the battery capacity has been estimated, a Lithium Ion battery arrangement is integrated. The battery module is integrated by 6 batteries of the Li-Ion-18650 series, each battery provides a voltage of 3.7 Vdc with a capacity of 2200 mAh. The set of batteries is configured in series reaching a total voltage of 22.2 V and a capacity of 13.2 Ah. This configuration allows you to have a cut-off voltage of 16.65 Vdc and a maximum of 25.84 Vdc, thus obtaining a nominal voltage of 24 V for the connection of the UAV subsystems.

The nominal discharge charts of the battery can be seen in Fig. 16. The nominal discharge area with a current of 5.7A is in a range of approximately 2 hours. However, in flight conditions with the peak load it can be observed that the discharge allows to have an autonomy of approximately 35 minutes.

To evaluate the behavior of the system under flight conditions, a simulation of the loading and unloading system of the storage system has been performed taking as a reference the flight profile throughout the day, presented in Fig. 17.

This has resulted in a flight time of approximately 3 hours from 100% SOC to 0% SOC with a voltage of 17 Volts. This can be seen in Fig. 18.

On the other hand, by implementing the storage system to a renewable energy source such as the photovoltaic system located on the wings of the aircraft, it has been possible to increase the flight autonomy to approximately 11 hours of flight, increasing the autonomy approximately 4 times in sunny day conditions with a flight starting at 8 am with its peak radiation at 12 hours. This allows to validate that the battery capacity obtained is the optimal one since it allows to increase the flight time, Fig. 19.

The optimal implementation of the storage system allows to reduce the weight of the UAV, which is directly related to its energy

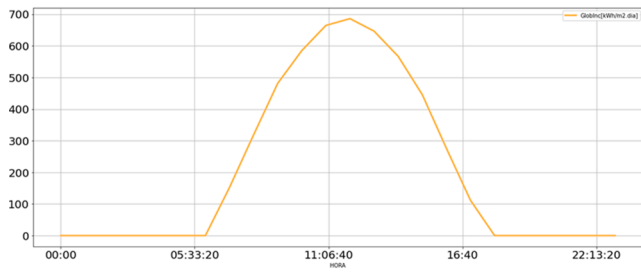


Fig. 14. Average temperature radiation for the most critical month of the year.

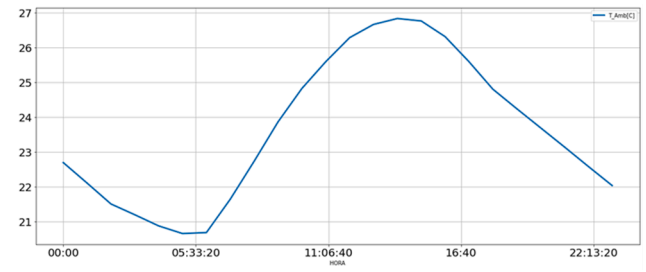


Fig. 15. Block diagram of the energy balance of the proposed system.

consumption, allowing to increase the flight autonomy. Similarly, it must be taken into account that the energy contribution of the photovoltaic system is limited by the UAV's wing area. The tests of the UAV system were conducted without the solar power system and with the system. The performance evaluation of the system without the integration of the Photovoltaic power source resulted in a cumulative flight duration of approximately 2.40 hours. Nevertheless, when the PV system was introduced, notwithstanding the addition of 690 g to the overall UAV weight, the flight duration exhibited a notable enhancement of approximately threefold. It should be noted that to achieve maximum performance, particularly optimal conditions regarding the received radiation by the solar cells at the test site have been sought, commencing the flight at approximately 10 am [31].

4. Conclusions

The main contribution of this research focuses on the optimization of the use of energy from a renewable system to power a fixed-wing UAV.

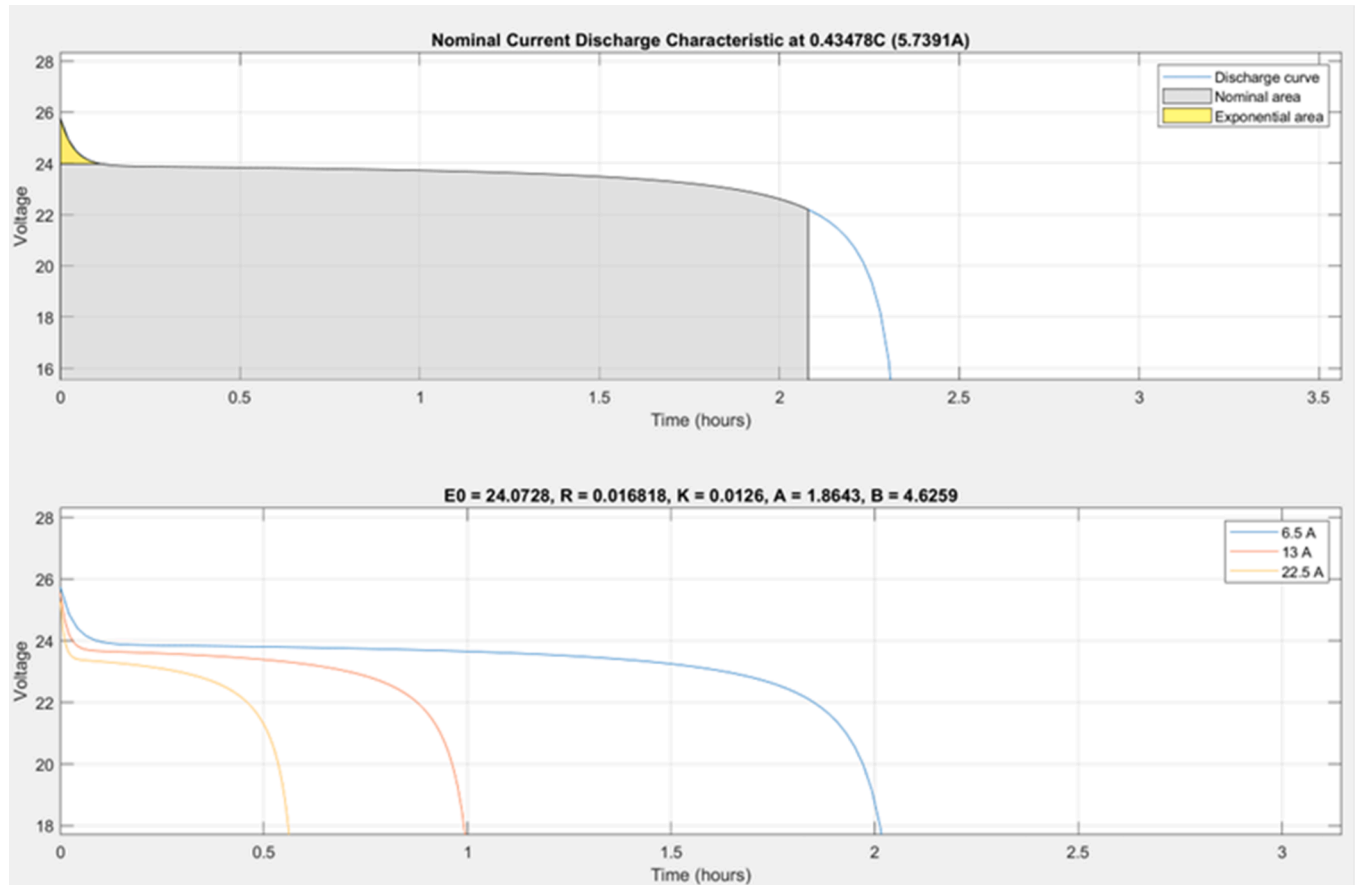


Fig. 16. Discharge characteristics of the battery bank.

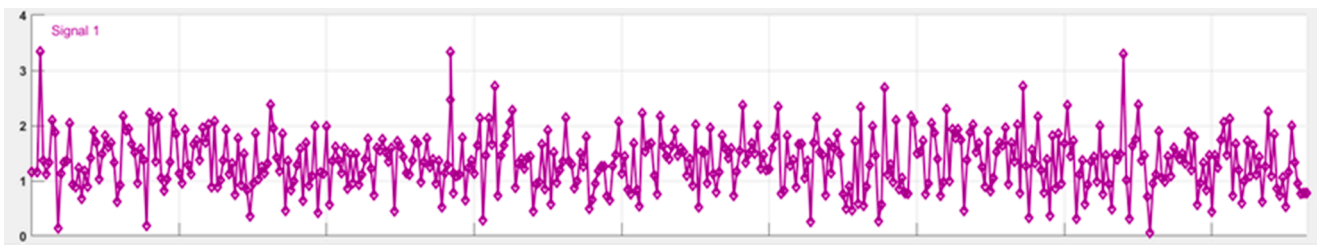


Fig. 17. Discharge profile based on flight over a day.

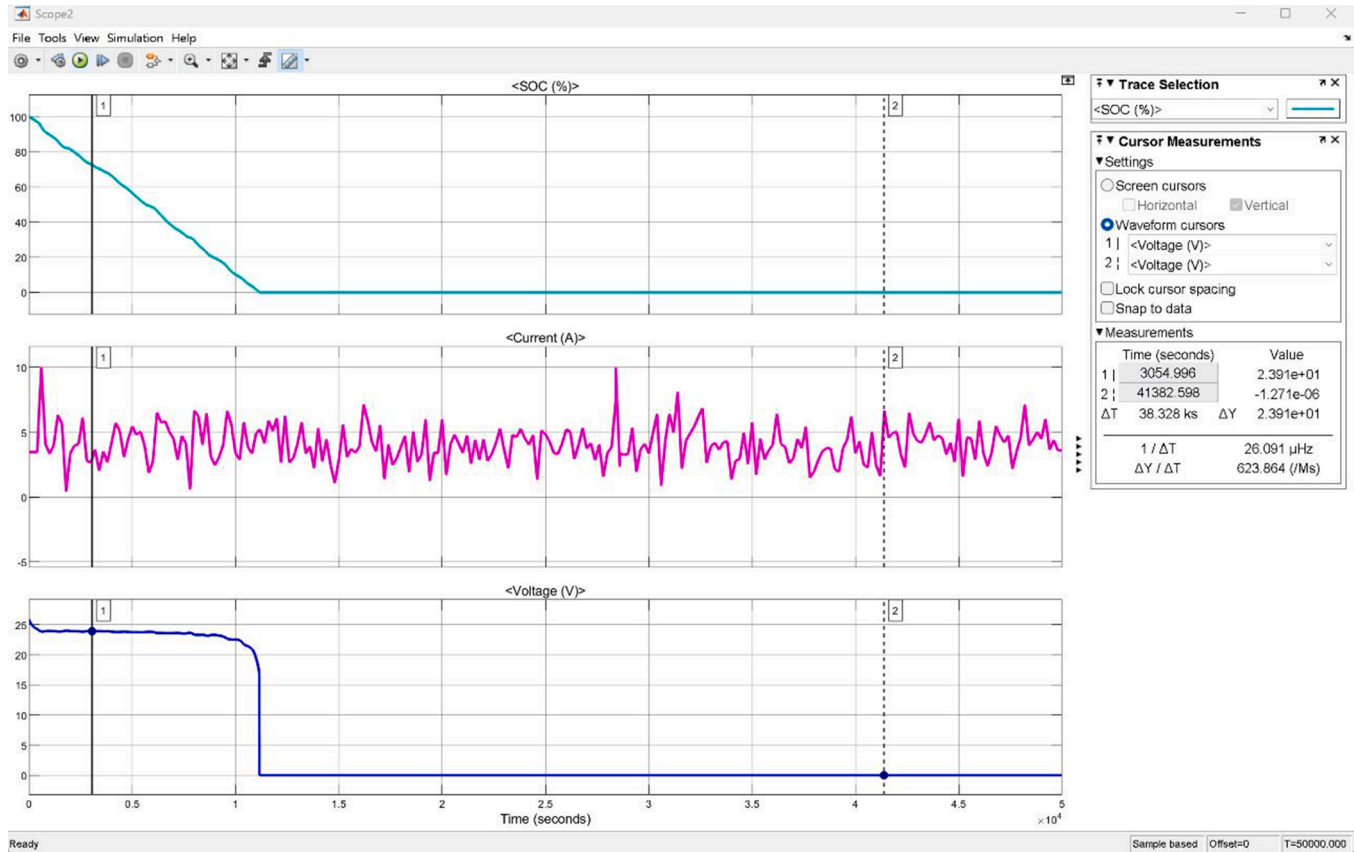


Fig. 18. Battery discharge behavior in reference to SOC, current, and voltage without the PV system.

For this purpose, the different components were analyzed, and a solar photovoltaic system was designed. The design and sizing of the photovoltaic system acting as a power source for the UAV was performed based on the flight mission test conditions.

The comprehensive analysis of meteorological conditions, encompassing variables such as irradiation, temperature, wind speed, wind direction, atmospheric pressure, and humidity, has enabled us to successfully validate the aerodynamic and energetic design through advanced software tools.

The use of tools such as FoilSim III, for the analysis of aerodynamic profiles with a low Reynolds number such as the DAE-5 Profile, N-60 Profile and the Selig Profile profiles such as Sa7038, S4083 and SG604, have allowed us to have a vision of the aerodynamic behavior of the UAV, of course. On the other hand, the use of MatLab for the simulation of different trajectories as well as the energy behavior regarding the loading and unloading of the battery, makes it possible to analyze the flight behavior of the UAV, in different flight conditions. This minimizes construction time and materials used in the design of the UAV. Battery analysis is important to predict the behavior of the UAV, where it is possible to observe the charge and discharge profile based on the energy

consumption of the UAV.

The battery analysis is a crucial component in predicting the behavior of UAVs. It enables the observation of the charge and discharge profile as a function of the energy consumption of the UAV. This analysis provides valuable insights into the energy management of UAVs, which is crucial for their efficient operation. The integration of C60 photovoltaic cells consolidates an optimal design for video surveillance applications, since it provides a stealthy vehicle with better autonomy.

The simulation has yielded valuable insights that have led to the identification of an objective function. This function is designed to optimize the charging capacity of the battery, which is essential to achieve longer flight times for aircraft, especially during video surveillance missions. By implementing this optimization technique, the system's autonomy capacity can be increased by up to four times, even without a photovoltaic backup. It's important to note that these results were evaluated under ideal conditions, with a clear sky and wind speeds lower than 3 m/s.

The future work involves enhancing the programming in the control propellers system, and system and integrating it with embedded systems for IoT communications.

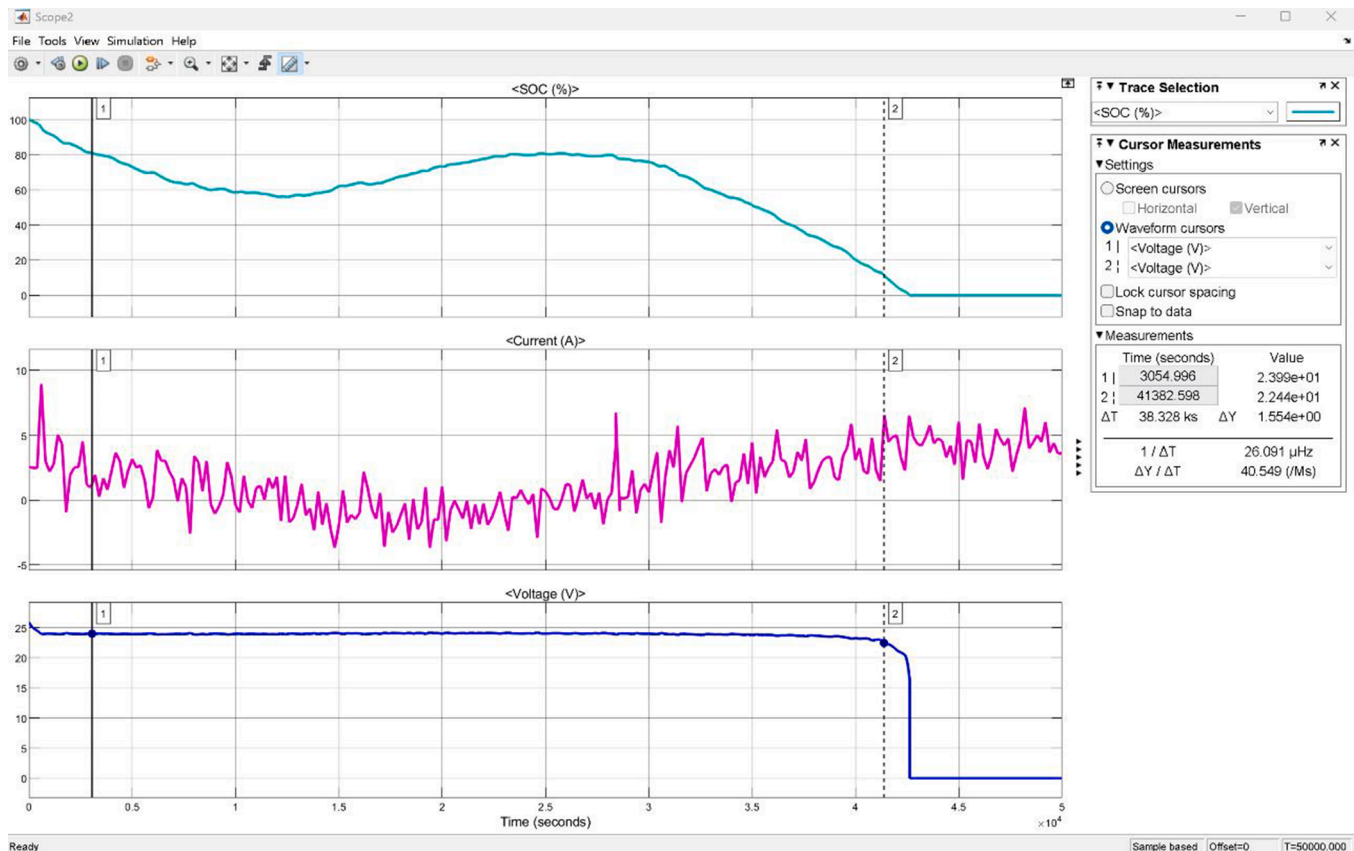


Fig. 19. Battery discharge behavior in reference to SOC, current, and voltage with the PV system.

CRedit authorship contribution statement

Franklin Salazar: Investigation. **Maria Sofia Martinez-Garcia:** Investigation. **Angel de Castro:** Investigation. **Nube Logroño:** Investigation. **Maria F. Cazorla-Logroño:** Investigation. **Jesús Guamán-Molina:** Investigation. **Carlos Gómez:** Investigation.

Declaration of Competing Interest

I have received research funding from DIDE Research and Development Directorate of the Technical University of Ambato for their special help in the development of this proposal, thanks to the financing of the Project "Design of a communications platform for technological applications of precision agriculture with Drones" We affirm that these potential conflicts of interest have not influenced the design, execution, or reporting of the research presented in this manuscript. Our commitment to maintaining the integrity and objectivity of the study remains uncompromised. We understand that the disclosure of conflicts of interest is essential for ensuring transparency and impartiality in scientific research. If any additional conflicts of interest arise during the peer-review process, we pledge to promptly inform the editorial team of Sustainable Futures. Thank you for considering our manuscript for publication. We appreciate the opportunity to contribute to the scholarly dialogue in the field of sustainable development.

Data availability

The authors do not have permission to share data.

Acknowledges

The Authors thank the DIDE Research and Development Directorate

of the Technical University of Ambato for their special help in the development of this proposal, thanks to the financing of the project "Design of a communications platform for technological applications of precision agriculture with Drones."

References

- [1] M.A. Bramantya, R.R.R. Ginting, Study of the effect of 4-digit NACA variation on airfoil performance using computation fluid dynamics, AIP Conf. Proc. 2248 (2020), 020002.
- [2] S. Junk, W. Schröder, S. Schrock, Design of Additively Manufactured Wind Tunnel Models for Use with UAVs, in: Procedia CIRP, volume 60, Elsevier, S241–246.
- [3] K.L. Pham, J. Leuchter, R. Bystricky, M. Andrie, N.N. Pham, V.T. Pham, The study of electrical energy power supply system for UAVs based on the energy storage technology; aerospace, 2022, 9, 9, 500.
- [4] J. Carvalho, L. Nascimento, M. Soares, N. Valério, A. Ribeiro, L. Faria, A. Silva, N. Pacheco, J. Araújo, C. Vilarinho, Life cycle assessment (LCA) of biochar production from a circular economy perspective, Processes 10 (12) (2022) 2684.
- [5] J.L. Hernandez-Toral, I. González-Hernández, R. Lozano, Sun tracking technique applied to a solar unmanned aerial vehicle, Drones 3 (2) (2019) 51.
- [6] P. Rajendran, H. Smith, Sensitivity analysis of design parameters of a small solar-powered electric unmanned aerial vehicle, J. Eng. Sci. Technol. 13 (12) (2018) 3922–3931.
- [7] M.N. Boukoberine, Z. Zhou, M. Benbouzid, A critical review on unmanned aerial vehicles power supply and energy management: solutions, strategies, and prospects, Appl. Energy 255 (2019) 113823.
- [8] L. Girlevicius, Evaluation of solar powered systems in small scale UAV designs.
- [9] G.E. G. Padilla, K.-J. Kim, K.H. Yu, S.-h. park, Flight path planning of solar-powered UAV for sustainable communication relay, IEEE Rob. Autom. Lett. 5 (4) (2020) 6772–6779.
- [10] P. Rajendran, H. Smith, Development of design methodology for a small solar-powered unmanned aerial vehicle, Int. J. Aerospace Eng. 2018 (2018).
- [11] B. Vera, B. Andrés, P. Castillo, W. Geovanny, Seguimiento y búsqueda de objetivos en entornos complejos usando micro vehiculos aéreos con cámaras monoculares para aplicaciones militares, 2020.
- [12] P.B. Montoya, R.V. Briones, Empleo de los UAV, en operaciones de seguridad y vigilancia en las áreas estratégicas en el Ecuador, Revista de Ciencias de Seguridad y Defensa 4 (4) (2019) 15–15.
- [13] M.H. Sadraey, Design of unmanned aerial systems, John Wiley & Sons, 2020.

- [14] J. Aerospace Technol. Manag. 8 (2016) 397–407. Design analysis of solar-powered unmanned aerial vehicle,
- [15] S. Arumbakkam, K. Brassard, P. Casey, L. Fahey, D. Hoddinott, T. Khan, E. Liu, Z. Lou, M. Moncton, Y. Olins, Design of an Intelligent Self-aware Solar-powered Unmanned Aerial Vehicle: Conventional and Unconventional Design Approaches. AIAA Scitech 2019 Forum, 2019, p. 0316.
- [16] D. Joshi, D. Deb, S. Muyeen, Comprehensive review on electric propulsion system of unmanned aerial vehicles, Front. Energy Res. (2022) 739.
- [17] H. Ahn, J. Ahn, Design and analysis of a solar-power mini-uav for extended endurance at low altitude, Int. J. Aeronaut. Space Sci. 20 (2019) 561–569.
- [18] O.D. Dantsker, M. Theile, M. Caccamo, Integrated Power Modeling for a Solar-powered, Computationally-intensive Unmanned Aircraft, 2020 AIAA/IEEE Electric Aircraft Technologies Symposium (EATS), 2020, pp. 1–21.
- [19] C. Thipyopas, V. Sripawadkul, N. Warin, Design and Development of a Small Solar-powered UAV for Environmental Monitoring Application, 2019 IEEE Eurasia Conference on IOT, Communication and Engineering (ECICE), 2019, pp. 316–319.
- [20] N. El-Atab, R.B. Mishra, R. Alshanbari, M.M. Hussain, Solar powered small unmanned aerial vehicles: a review, Energy Technol. 9 (2021) 2100587.
- [21] Y. Chu, C. Ho, Y. Lee, B. Li, Development of a Solar-Powered Unmanned Aerial Vehicle for Extended Flight Endurance, Drones 5 (2) (2021) 44.
- [22] X. Dai et al, Energy-efficient UAV communications in the presence of wind: 3d modeling and trajectory design, ArXiv preprint arXiv:2304.06909.
- [23] T.B. Glick, M.A. Figliozzi, A. Unnikrishnan, Case study of drone delivery reliability for time-sensitive medical supplies with stochastic demand and meteorological conditions, Transp. Res. Record 2676.1 (2022) 242–255.
- [24] S.G. Kontogiannis, J.A. Ekaterinaris, Design, performance evaluation and optimization of a UAV, Aerosp. Sci. Technol. 29 (1) (2013) 339–350.
- [25] G. de Carvalho Bertoli, G.M. Pacheco, G.J. Adabo, Extending Flight Endurance of Electric Unmanned Aerial Vehicles through Photovoltaic System Integration. 2015 International Conference on Renewable Energy Research and Applications (ICRERA), 2015, pp. 143–147.
- [26] A.O. Baba, G. Liu, X. Chen, Classification and evaluation review of maximum power point tracking methods, Sustain. Futures 2 (2020) 100020.
- [27] Q. Chen, C. Wachenheim, S. Zheng, Land scale, cooperative membership and benefits information: unmanned aerial vehicle adoption in china, Sustain. Futures 2 (2020) 100025.
- [28] K. Oladeja, A. Alabi, Y. Dambatta, Aerodynamic performance analysis of an optimized aerofoil for unmanned aerial vehicles, Res. Square (2023).
- [29] D. Liviu, J. Corcau, D. Voinea, Solar UAVs-more aerodynamic efficiency or more electrical power, Energies 16.9 (2023).
- [30] Q. Chen, C. Wachenheim, S. Zheng, Efficiency decreases in a laminated solar cell developed for a UAV, Materials 15.24 (2022) 8774.
- [31] P.I. Chulde, J.R. Gómez, Design and construction of a UAV for strategic missions of the FAE research center using solar panels, Bachelor's thesis, Universidad Técnica de Ambato. Faculty of Systems Engineering, Electronics and Industrial Engineering. Degree in Electronics and Communications (2022).
- [32] E. Cetinsoy, C. Hancer, K.T. Oner, E. Sirimoglu, M. Unel, Aerodynamic design and characterization of a quad tilt-wing UAV via wind tunnel tests, J. Aerosp. Eng. 25 (4) (2012) 574–587.
- [33] A.Z. Ruiz, C.P. Ferreira, 13. drones: technology available to health and safety, Www.congreso.prevenconar.com.
- [34] M.H. Sadraey, Design of unmanned aerial systems, John Wiley, Sons, 2020.
- [35] P. Panagiotou, P. Kaparos, C. Salpingidou, K. Yakinthos, Aerodynamic design of a MALE UAV, Aerosp. Sci. Technol. 50 (2016) 127–138.
- [36] D. Dantsker, Johnson, Development and initial testing of the aero testbed: a large-scale unmanned electric aerobatic aircraft for aerodynamics research, 31st AIAA Appl. Aerodyn. Conf. (2013) 2807.
- [37] A. Abdullah, Qassim, Classification of the unmanned aerial systems. pennsylvania state, 2014, Pennsylvania State, Available: <https://www.e-education.psu.edu/geog892/node/5>. [Accessed 21 April 2021].
- [38] A. Gutiérrez, Optimización paramétrica de la aerodinámica de un formula student con virtual wind tunnel, BS Thesis (2017).
- [39] D.A. Puerto, O.D. López, Simulación del Flujo Alrededor de un Perfil ALAR NACA 4415 con un Flap Tipo Gurney, Mecánica Computacional, Puerto, 2020.
- [40] S. Paz, The wing profile and its NACA nomenclature, Ciencia y poder aéreo 8.1 (2013) 26–32.